

Degradation of the BAF Complex Factor BRD9 by Heterobifunctional Ligands

David Remillard, Dennis L. Buckley, Joshiawa Paulk, Gerard L. Brien, Matthew Sonnett, Hyuk-Soo Seo, Shiva Dastierdi, Martin Wühr, Sirano Dhe-Paganon, Scott A. Armstrong, and James E. Bradner*

Abstract: The bromodomain-containing protein BRD9, a subunit of the human BAF (SWI/SNF) nucleosome remodeling complex, has emerged as an attractive therapeutic target in cancer. Despite the development of chemical probes targeting the BRD9 bromodomain, there is a limited understanding of BRD9 function beyond acetyl-lysine recognition. We have therefore created the first BRD9-directed chemical degraders, through iterative design and testing of heterobifunctional ligands that bridge the BRD9 bromodomain and the cereblon E3 ubiquitin ligase complex. Degradors of BRD9 exhibit markedly enhanced potency compared to parental ligands (10- to 100-fold). Parallel study of degradors with divergent BRD9-binding chemotypes in models of acute myeloid leukemia resolves bromodomain polypharmacology in this emerging drug class. Together, these findings reveal the tractability of non-BET bromodomain containing proteins to chemical degradation, and highlight lead compound **dBRD9** as a tool for the study of BRD9.

Small-molecule inhibitors of BRD4 established the feasibility of inhibiting acetyl-lysine recognition domains (bromodomains).^[1] The broad use of the chemical probe JQ1 and other inhibitors of the bromodomain and extra-terminal domain (BET) subfamily of transcriptional co-activators has

contributed an enhanced mechanistic understanding of gene control and has availed new therapeutic opportunities in cancer.^[2,3] Indeed, multiple BET inhibitor candidates from several groups are now undergoing clinical trials for diverse indications in and outside of oncology.^[4-6] Further, significant research effort has contributed a number of high quality chemical probes for bromodomain-containing proteins beyond the BET family.^[7,8]

The bromodomain-containing protein BRD9 has garnered particular attention as a component of the human ATP-dependent chromatin remodeling BAF complex (also known as SWI/SNF). Meta-analyses of whole-genome sequencing efforts have recently identified a high frequency of recurrent somatic mutations in BAF factors in diverse human cancers.^[9] Within several subsets of these genetically defined malignancies, components of the BAF complex have emerged as context-specific dependencies, either supporting growth within a residual complex following loss of function mutation, or as novel oncogenes such as the SS18-SSX fusion.^[10] These observations have generated interest in therapeutic strategies to target BAF.

Beyond its presence in the BAF complex, a lack of functional annotation for BRD9 has provided incentive for development of BRD9 selective inhibitors to interrogate its biological role and to assess any therapeutic potential. Several BRD9-directed efforts in discovery chemistry have been reported,^[11-15] developing chemotypes for BRD9-specific engagement. Further, a recent study implicated BRD9 as a dependency in acute myeloid leukemia (AML), where bromodomain inhibition prompted a cytostatic response.^[16] Beyond the bromodomain, the function of BRD9 remains unclear, and chemical tools to study other functions of BRD9 are not available. We therefore undertook to create first chemical probes that destabilize BRD9, anticipating that the study of acute BRD9 loss would offer a powerful approach to interrogate BAF complex function.

Recently, we reported a strategy to direct protein-specific degradation using bifunctional molecules to recruit the cereblon (CRBN) ubiquitin ligase complex to non-physiologic protein substrates,^[17] providing an all-chemical solution to prior efforts using peptides to bridge E3 ligases and ligand targets (PROTACs).^[18,19] In our prior research, we directed the degradation of BET family proteins by appending CRBN ligands to JQ1, resulting in rapid and potent degradation of BRD2, BRD3, and BRD4. These findings have been well validated, suggesting a broader utility of this strategy.^[20-22]

Toward the elaboration of BRD9-directed degradors, we initially evaluated putative pharmacophores from reported

[*] D. Remillard, Dr. D. L. Buckley, Dr. J. L. Paulk, S. Dastierdi, Dr. J. E. Bradner
Department of Medical Oncology, Dana-Farber Cancer Institute
Boston, MA (USA)
E-mail: james_bradner@dfci.harvard.edu
james.bradner@novartis.com

Dr. G. L. Brien, Dr. S. A. Armstrong
Department of Pediatric Oncology, Dana-Farber Cancer Institute
Boston, MA (USA)

M. Sonnett
Department of Systems Biology, Harvard Medical School
Boston, MA (USA)

M. Sonnett, Dr. M. Wühr
Lewis-Sigler Institute for Integrative Genomics, Princeton University
Princeton, NJ (USA)

Dr. H.-S. Seo, Dr. S. Dhe-Paganon
Department of Cancer Biology, Dana-Farber Cancer Institute
Boston, MA (USA)

Dr. M. Wühr
Department of Molecular Biology, Princeton University
Princeton, NJ (USA)

Supporting information and the ORCID identification number(s) for the author(s) of this article can be found under:
<https://doi.org/10.1002/anie.201611281>.

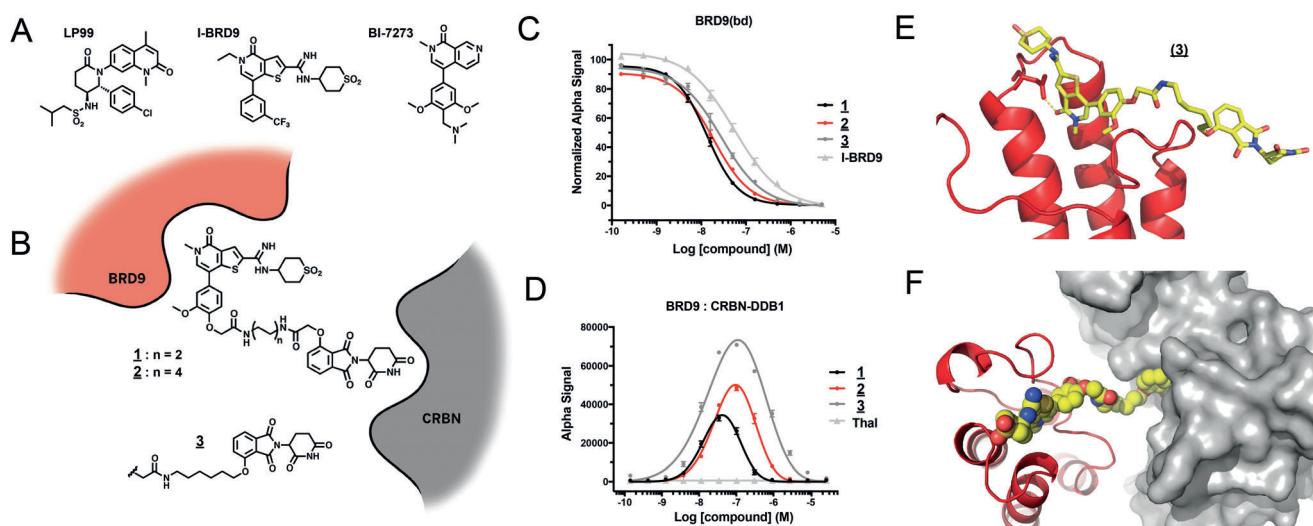


Figure 1. Design and characterization of thienopyridinone BRD9-targeted degraders. A) Structures of select BRD9 bromodomain probes. B) Schematic representation of degrader design. C) Vehicle-normalized BRD9(bd) displacement (AlphaScreen quadruplicate means \pm SEM). D) Compound-induced ternary complex formation of recombinant BRD9(bd) and CRBN–DDB1 (AlphaScreen quadruplicate means \pm SEM). E) Cocrystal structure of **3** with BRD9(bd) (PDB 5TWX). F) Docking of (E) into the published CRBN–DDB1 structure (4CI3).

bromodomain probes LP99 and I-BRD9, and subsequently expanded our study to a third probe, BI7273, reported during the course of this research (Figure 1 A).^[12,14,15] To explore the potential of bifunctional derivatives to induce BRD9 degradation, we initially selected as our starting point a close chemical analog of I-BRD9 described by GlaxoSmithKline (GSK-39).^[14] This ligand was attractive in that it offered high binding affinity ($IC_{50} = 7.9$ nM) as well as a solvent exposed methoxy substituent amenable to chemical derivatization. In our initial design strategy, we adapted this ligand by installing an ether-linked acetyl moiety as a handle for E3 ligand attachment, as exemplified by compounds **1–3** (Figure 1 B). Using this approach, we prepared a series of analogs that differ in linker length and composition, and explored varied attachment chemistries to CRBN or von Hippel–Lindau (VHL) E3 ligase ligands (Table S1 in the Supporting Information).

To characterize these compounds biochemically, we developed competitive ligand binding assays to the BRD9 bromodomain and the co-purified CRBN–DDB1 complex. High BRD9 affinity was retained across all compounds of this series relative to the parental bromodomain ligand, as exemplified by IC_{50} values for compounds **1–3** that closely approximate the published IC_{50} for GSK-39 (7.9 nM; Figure 1 C, Table S1). Moderate differences were observed in CRBN–DDB1 affinity among compounds with divergently linked phthalimides (Table S1). For example, the direct alkyl ether phthalimide linkage of **3** showed slightly improved binding over acetamide ethers **1** and **2**. Interestingly, measured affinities of all compounds exceeded that of unmodified thalidomide, perhaps reflecting positive affinity contributions of the pendant linker substituents.

To elicit protein degradation, bifunctional molecules must be able to efficiently associate the E3 ligase with the target. To measure this activity, we developed a homogenous luminescence assay to report on compound-induced proximity of

BRD9 and CRBN. All of the bifunctional compounds in our initial series were able to significantly induce proximity of the BRD9 bromodomain and CRBN–DDB1 relative to unmodified thalidomide; an activity subsequently referred to simply as “dimerization” (Figure 1 D, Table S1). This ternary interaction exhibited a characteristic auto-inhibitory concentration dependence consistent with bimolecular interactions dominating at saturating ligand concentrations.^[23]

Across a range of concentrations, the intermediate length alkyl ether analog **3** afforded robust dimerization. To understand BRD9 recognition by this compound, we solved a cocrystal structure with the BRD9 bromodomain. The pose adopted by the bromodomain warhead confirmed a conserved binding mode relative to the free probe, with the derivatized methoxy position projected to solvent as envisioned (Figure 1 E, Figure S1). In-silico modeling of the ternary assembly including CRBN–DDB1 demonstrated the steric feasibility of ternary formation, with the two ligand-binding domains brought into close assembly by compound **3** (Figure 1 F).^[24]

To evaluate the ability of these compounds to degrade BRD9 in a cellular context, we treated a human AML cell line (MOLM-13) for 4 hours at varied concentrations and assessed BRD9 protein levels by immunoblot. While **1** and the extended PEG-linked **S1** (see supplement) had little effect on BRD9 protein abundance, marked BRD9 loss was observed with the more potent biochemical dimerizers **2** and **3** (Figure 2 A, Table S1). Encouraged by this activity, we prepared an additional focused set of analogs exploring various molecular features. We examined the effect of linker rigidity by installing a conformationally constrained bipiperidine linker in compound **S2**. This molecule showed significant improvement in both dimerization and cellular potency, possibly by enforcement of an extended ternary-competent linker conformation (Table S1). To pursue degradation by alternate E3 ligases, we prepared the VHL-ligand

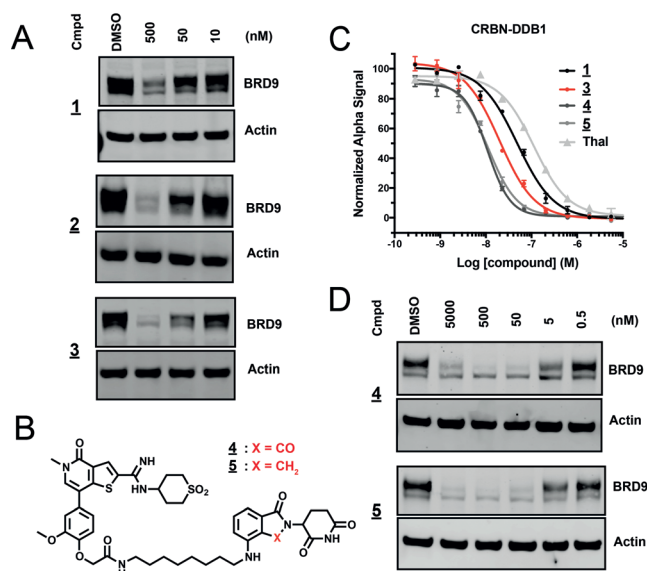


Figure 2. Performance of thienopyriminone degraders. A) Immunoblot for BRD9 and actin after 4 hour treatment of MOLM-13 with indicated concentrations of **1**, **2**, and **3**. B) Chemical structures of **4** and **5**. C) Vehicle-normalized CRBN-DDB1 displacement (AlphaScreen quadruplicate means \pm SEM). D) Immunoblot for BRD9 and actin after 4 hour treatment of MOLM-13 with indicated concentrations of **4** and **5**.

conjugates **S3** and **S4**; however, these were found to be ineffective (Table S1).

Additional analogs explored substitution of the phenolic attachment as found in **3** for the amine type linkages found in compounds **S5**, **4**, and **5** (Figure 2B, Table S1). These compounds tightly bound CRBN, and effectively induced degradation of BRD9 (Figure 2C,D). The lenalidomide-based analog **5** showed the best overall performance, effectively downregulating BRD9 protein over a broad range of concentrations. We therefore selected this molecule for further characterization.

To evaluate the kinetics of BRD9 degradation, we exposed MOLM-13 cells to **5** at a fixed concentration (100 nM) and assessed BRD9 abundance over time by immunoblot. Near complete BRD9 loss was observed within 1 hour, with no detectable return observed for the duration of the 24-hour treatment period (Figure 3A). This profile is appropriate to enable study of primary consequences of acute BRD9 loss, as well as viability defects manifested over longer periods.

To interrogate the mechanism of degradation by compound **5** in a cellular context, we assessed the requirement for target binding, proteasome activity, and activated cullin E3 ligases via chemical and genetic perturbations (Figure 3B,C). Pretreatment with excess I-BRD9 or lenalidomide competed with **5** for binding to BRD9 or CRBN, respectively, and prevented degradation, consistent with a requirement for intracellular engagement of both targets (Figure 3B).

Degradation was abolished by the co-treatment with the proteasome inhibitor carfilzomib, confirming a requirement for proteasome function. Pretreatment using a mechanism-based inhibitor of neddylation also rescued BRD9 levels, as

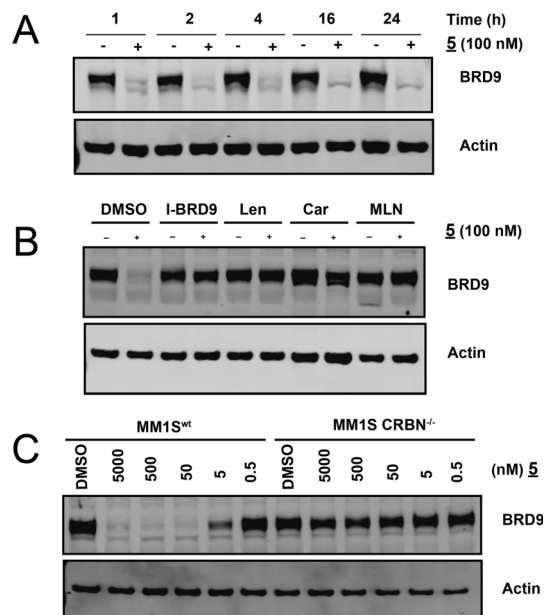


Figure 3. Temporal and mechanistic characterization of BRD9 degradation by **5**. A) Immunoblot for BRD9 and actin after treatment of MOLM-13 Cells with 100 nM **5** for the indicated times. B) Immunoblot for BRD9 and actin after a 4 h pre-treatment of MM.1S cells with vehicle, I-BRD9, Lenalidomide, Carfilzomib,^[9] or MLN-4924, followed by a 2-hour treatment with **5** (100 nM). [⁹] Car pretreatment 30 min. C) Immunoblot for BRD9 and actin after 4 hour treatment with **5** at the indicated doses in MM.1S^{wt} or MM.1S^{CRBN-/-} cells.

expected given the requirement for neddylation of CRL E3 ligases for activity.^[25,26] We further established a requirement for CRBN by examining the effects of compound **5** treatment in cells rendered CRBN deficient by CRISPR/Cas9 (CRBN^{-/-}). While treatment of wild type MM.1S cells resulted in marked dose-dependent BRD9 loss, treatment of the paired MM.1S CRBN^{-/-} line failed to induce BRD9 degradation (Figure 3C).^[27] These data support CRBN- and proteasome-dependent degradation of BRD9 by **5**.

We aimed to further characterize **5** by establishing the biochemical selectivity profile among 32 representative members of the human bromodomain family. While the results of this analysis confirmed potent engagement of BRD9, we also observed substantial off-target binding activity, notably including BET bromodomains (Figure 4A). Because of the confounding transcriptional and anti-proliferative effects associated with BET inhibition or loss, we felt selectivity over this family to be an important concern. At this stage of research, the concurrent publication of BI-7273, a highly selective BRD9 probe from Boehringer Ingelheim,^[14,15] inspired exploration of a novel chemical series of bifunctional degraders (Table S2).

Compound **6** (**dBRD9**), a PEG-linked pomalidomide conjugate, was found to prompt rapid BRD9 degradation over a broad range of concentrations (Figure 4B,C). Gratifyingly, **dBRD9** also showed an improved bromodomain engagement profile, with reduced binding activity across the BET family (Figure 4D). A comparison of biochemical affinity of **5** and **dBRD9** for the BET bromodomain, BRD4-

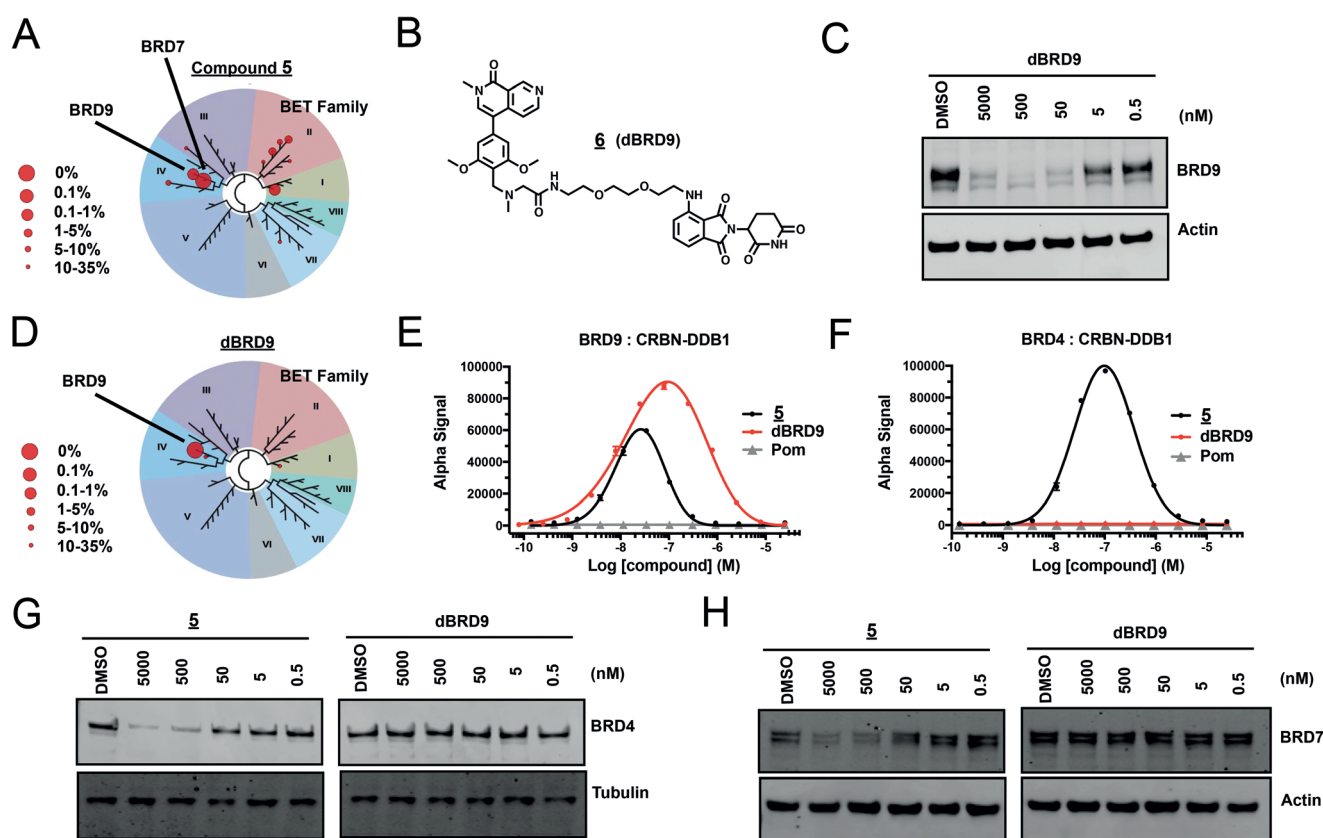


Figure 4. Naphthiridinone degrader **6** (**dBRD9**) offers improved biochemical and cellular selectivity. A) Selectivity of phage-displayed bromodomain displacement by **5** (Bromoscan). B) Chemical structure of **dBRD9**. C) Immunoblot of BRD9 and actin after 4 h treatment of MOLM-13 cells with indicated concentrations of **dBRD9**. D) Selectivity of phage-displayed bromodomain displacement by **dBRD9** (Bromoscan). E) Compound-induced ternary complex formation of recombinant BRD9(bd) and CRBN–DDB1 (AlphaScreen quadruplicate means \pm SEM). F) Compound-induced ternary complex formation of recombinant BRD4(1) and CRBN–DDB1 as in (E). G) Immunoblot for BRD4 and actin after 4 h treatment of MOLM-13 cells with indicated concentrations of **5** or **dBRD9**. H) Immunoblot for BRD7 following treatment as in (G).

(1), by competitive ligand displacement confirmed this result (Figure S2). Moreover, while **5** was able to effectively induce biochemical association of CRBN–DDB1 with either BRD9 or BRD4, **dBRD9** lost all ability to dimerize BRD4 with CRBN–DDB1 above background levels, but retained robust dimerization of BRD9 (Figure 4E,F). Consistent with this result, **dBRD9** showed improved cellular selectivity. Off-target degradation activity on BRD4 and BRD7, observed at high concentrations of **5**, was not detectable by western blot following **dBRD9** treatment (Figure 4G,H).

To assess the cellular selectivity for BRD9 degradation in an unbiased, quantitative manner, we measured effects of **dBRD9** (100 nM for 2 hours) versus vehicle (DMSO) on all cellular proteins in MOLM-13 cells detected by isobaric tagging and mass spectrometry.^[28] Strikingly, of the 7326 proteins quantified in this experiment, BRD9 was the singular protein showing a marked and statistically significant difference in abundance, showing a median 5.5 fold lower abundance in **dBRD9** treated samples (FDR corrected q -value < 0.01) (Figure 5). Levels of other proteins were remarkably static between treatments with 99% of proteins differing less than 0.30-fold. Consistent with quantification by western blot, no significant change in BRD4 or BRD7 levels was observed.

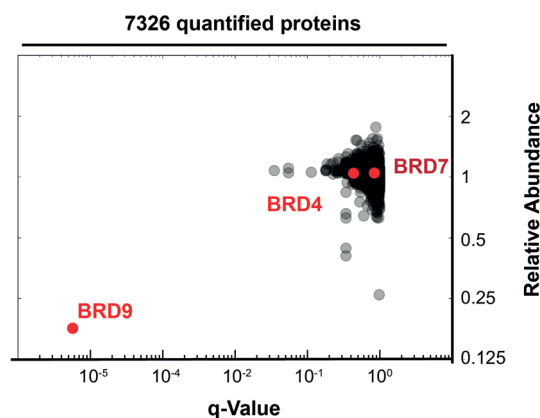


Figure 5. **dBRD9** selectivity established by whole-cell lysate proteomics. Fold change in relative abundance of 7326 proteins quantified from MOLM-13 cells treated for two hours with **dBRD9** (100 nM) or vehicle (DMSO), versus q -value for quintuplicate replicates.

Having characterized two potent and pharmacologically distinct degraders of BRD9, we next sought to evaluate the anti-proliferative activity of these molecules in comparison to the parental bromodomain inhibitors. In the context of human AML lines (EOL-1, MOLM-13, MV4;11), compound

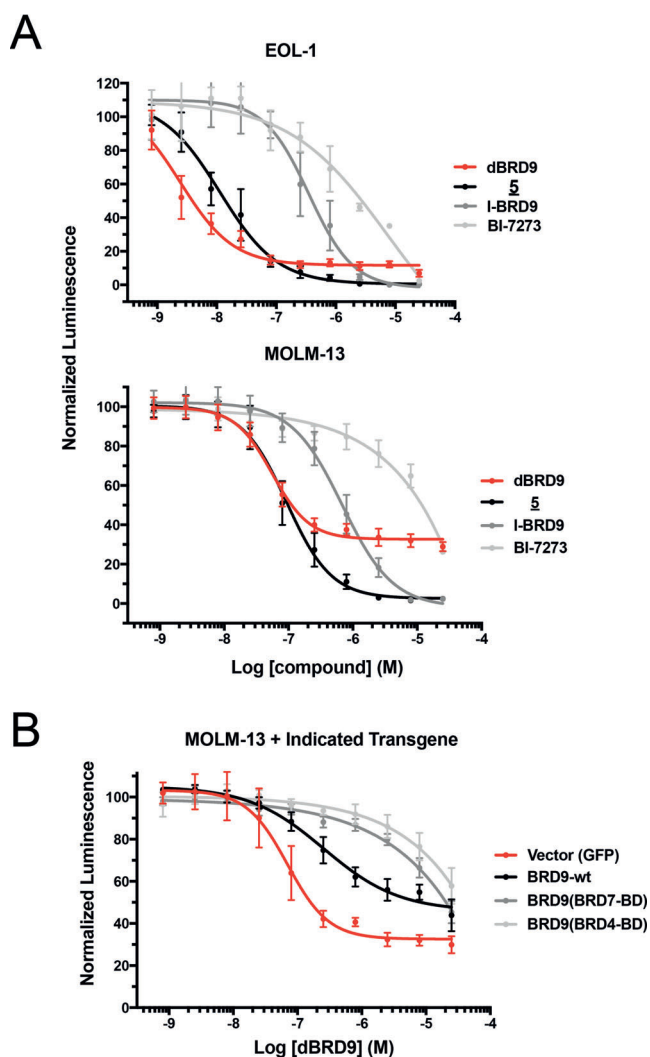


Figure 6. Impact of BRD9 degradation on cultured human leukemia lines. A) Viability of EOL-1 and MOLM-13 cell lines treated for 7 days with the indicated compounds (ATP-Lite quadruplicate means \pm SEM). B) Viability of MOLM-13 AML treated with **dBRD9** and measured as in (A) following transduction with recombinant BRD9 alleles or vector control.

5 and **dBRD9** both exerted a potent anti-proliferative effect, exceeding non-degrading probe potencies in excesses of 10- to 100-fold (Figure 6 A, Figure S3). Interestingly, although these two compounds exhibited comparable low nanomolar half-maximal anti-proliferative concentrations, the maximal effect (E_{max}) of **5** exceeded that of **dBRD9**, likely owing to the polypharmacology associated with **5**, particularly activity on BRD4, a well described AML dependency.^[17] These data argue that polypharmacologic degraders are a viable chemical strategy, and further demonstrate the ability of cereblon ligand conjugation to reveal relevant cellular off-target activities of chemical probes.

To further scrutinize the conclusion that the observed growth defect results from on-target activity of **dBRD9**, we extended the bromodomain-swap strategy of the Vakoc laboratory, who found that substitution of BRD4 or BRD7 bromodomains for the endogenous BRD9 domain produced

recombinant BRD9 alleles that lost affinity to BI-7273, but could functionally substitute for the wild type protein. We therefore stably transduced MOLM-13 cells with wild type BRD9, bromodomain substituted BRD9 alleles, or a GFP vector control, and re-evaluated sensitivity to **dBRD9** in the presence of each transgene. In both lines expressing domain-swap alleles, the anti-proliferative effect of **dBRD9** was dramatically rescued relative to vector control. Viral expression of exogenous wild type BRD9 also shifted sensitivity, but to an intermediate degree, consistent with retained susceptibility to **dBRD9**-induced degradation. These responses are fully congruent with the observed activity of **dBRD9** in each line by western blot (Figure S4 A). Consistent with its polypharmacology, the activity of compound **5** was only partially shifted by domain-swapped alleles, while the BRD9 independent activity of BET inhibitor JQ1 was wholly unaffected (Figure S4 B). Together with expression proteomics, these data provide extensive support that the observed sensitivity in MOLM-13 is a BRD9 specific effect.



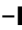

In the course of our on-target validation work, we prepared a non-targeting control analog (compound **S10**), which lacks a key hydrogen bonding moiety while being otherwise structurally identical to **dBRD9** (Figure S5 A). As expected, this molecule lost biochemical BRD9 bromodomain affinity, the ability to degrade BRD9, and accordingly, lost anti-proliferative activity in MOLM-13 (MOLM-13 IC₅₀ > 10 μ M) (Figure S5 B–D). Unexpectedly however, **S10** retained considerable activity in the multiple myeloma derived MM.1S line, which we had identified as **dBRD9** sensitive in studies of activity outside AML (Figure S5 E). Contemplating the known activity of IMiDs in MM.1S,^[27] we were lead to discover that **S10** and **dBRD9** retain activity against the IKZF family of lineage specific transcription factors; an activity not previously observed with **dBET-1** (Figure S5 F).^[17] We therefore caution that in select cell lines of lymphoid origin that express and depend on IKZF family proteins, researchers should control for this feature. We suspect that published molecules featuring similar CRBN targeting chemistry may also retain activity.

In summary, the present work describes the design and characterization of first-in-class chemical degraders of BRD9. These studies demonstrate the utility of the targeted degradation strategy to bromodomain-containing proteins beyond the BET family. This is particularly relevant, as competitive bromodomain inhibition has previously failed to phenocopy the effects of protein knock-down (shRNA) or knock-out (CRISPR-Cas9) for non-BET bromodomain proteins.^[29] Thus, using comparative biochemical and biological assays, we have qualified a lead BRD9 chemical degrader, **dBRD9**, as a selective probe useful for the study of BAF complex biology. The rapid and potent activity of this compound render it ideally suited to the study of fast biological responses such as transcriptional effects and nucleosome positioning. Finally, potent activity of **dBRD9** in cellular models of human AML is confirmed to be on target through expression proteomics, alongside chemical and genetic controls within the exemplar MOLM-13 line.

Communications



Protein Degraders

D. Remillard, D. L. Buckley, J. L. Paulk,
G. L. Brien, M. Sonnett, H.-S. Seo,
S. Dastierdi, M. Wühr, S. Dhe-Paganon,
S. A. Armstrong,
J. E. Bradner*    

Degradation of the BAF Complex Factor
BRD9 by Heterobifunctional Ligands

With structural guidance alongside comparative biochemical and biological assays, an iterative design strategy resulted in the development of small-molecule protein degraders that rapidly, potently, and selectively eliminate

bromodomain-containing protein BRD9 from the BAF complex. These first in class non-BET bromodomain degraders show significant potency improvements over existing BRD9 probes in models of acute myeloid leukemia.

